INVITED PAPERS

Suppression of nonlinear frequency-sweeping of resonant interchange modes in a magnetic dipole with applied radio frequency fields[a)]

D. Maslovsky,[b)] B. Levitt, and M. E. Mauel
Department of Applied Physics and Applied Mathematics, Columbia University, New York, New York 10027

(Received 14 November 2002; accepted 3 January 2003)

Interchange instabilities excited by energetic electrons trapped by a magnetic dipole nonlinearly saturate and exhibit complex, coherent spectral characteristics and frequency sweeping [H. P. Warren and M. E. Mauel, Phys. Plasmas **2**, 4185 (1995)]. When monochromatic radio frequency (rf) fields are applied in the range of 100–1000 MHz, the saturation behavior of the interchange instability changes dramatically. For applied fields of sufficient intensity and pulse-length, coherent interchange fluctuations are suppressed and frequency sweeping is eliminated. When rf fields are switched off, coherent frequency sweeping reappears. Since low frequency interchange instabilities preserve the electron's first and second adiabatic invariants, these observations can be interpreted as resulting from nonlinear resonant wave–particle interactions described within a particle phase-space, (ψ,φ), comprised of the third adiabatic invariant and the azimuthal angle. Self-consistent numerical simulation is used to study (1) the nonlinear development of the instability, (2) the radial mode structure of the interchange instability, and (3) the suppression of frequency sweeping. When the applied rf heating is modeled as an ''rf collisionality,'' the simulation reproduces frequency sweeping suppression and suggests an explanation for the observations that is consistent with Berk and co-workers [H. L. Berk *et al.*, Phys. Plasmas **6**, 3102 (1999)]. © *2003 American Institute of Physics.* [DOI: 10.1063/1.1557072]

I. INTRODUCTION

Collisionless dynamics of energetic particles are important to many phenomena in magnetized plasma such as those found in the radiation belts of magnetospheres,[1] toroidal magnetic fusion devices,[2] and laboratory terrella.[3–5] When strong magnetic fields separate the frequencies of the three characteristic periodic motions, cyclotron, ω_c, bounce, ω_b, and magnetic drift, ω_d, energetic wave–particle interactions with low-frequency perturbations can be described with a guiding-center drift Hamiltonian.[8] Low-frequency interchange modes that are resonant with the particle drift motion, $\omega \sim m\omega_d$, cause the third adiabatic invariant, ψ, to evolve in time. Since $\omega \ll \omega_b \ll \omega_c$, the first two adiabatic invariants, μ and J, remain constant even when the radial transport is chaotic.[6] Drift-resonance with interchange modes within a magnetic dipole provide an especially convenient geometry for the study of nonlinear wave–particle dynamics. This is because particle motion is described in the reduced phase-space coordinates of a one-dimensional system, (ψ,φ), that are simultaneously the physically-observable magnetic coordinates of the dipole, $\mathbf{B}=\nabla\psi\times\nabla\varphi$.

Recently, Berk and co-workers[7] described the occurrence of spontaneous frequency sweeping after a period of explosive growth of resonant particle instability near threshold.[9–11] Resonant particle instabilities with linear growth rates, γ_L, that are only marginally larger than their rates of nonresonant dissipation, γ_d, exhibited unexpected behaviors at saturation. Kinetic simulations showed the spontaneous formation of phase-space structures, ''holes'' and ''clumps,'' provided the dynamics of the resonant particles were sufficiently collisionless. The ''holes'' and ''clumps'' corresponded, respectively, to rising and falling tones with frequency sweeping proceeding in time approximately as $\sqrt{\gamma_d t}$. The saturated level of the instability lasted much longer than the nonresonant damping time, $1/\gamma_d$, because the ''holes'' and ''clumps'' moved through phase-space and allowed the continued release of energy by passing particles.

Small resonant particle collisionality is a necessary condition for frequency sweeping to occur. Berk and co-workers[7] define ν_{eff}^3 as the Fokker–Planck coefficient for stochastic resonant particle diffusion in the single phase-plane of the nonlinear wave–particle interaction. When $\nu_{\mathrm{eff}} > \gamma \equiv \gamma_L - \gamma_d$, collisional effects do not allow ''holes'' and ''clumps'' to form. Instead, frequency sidebands are formed and the mode amplitude becomes chaotic.[9,10] This regime describes observations of the saturation of Alfvén eigenmodes driven by fast ions trapped in a tokamak.[15,16] The strongly nonlinear regime characterized by explosive growth and followed by coherent frequency sweeping is predicted to occur only when $\nu_{\mathrm{eff}}/\gamma < 1$.

In this article, we present details of the first observations of the suppression of frequency sweeping by the application

[a)]Paper QI2 4, Bull. Am. Phys. Soc. **47**, 250 (2002).
[b)]Invited speaker. Electronic mail: dm341@columbia.edu

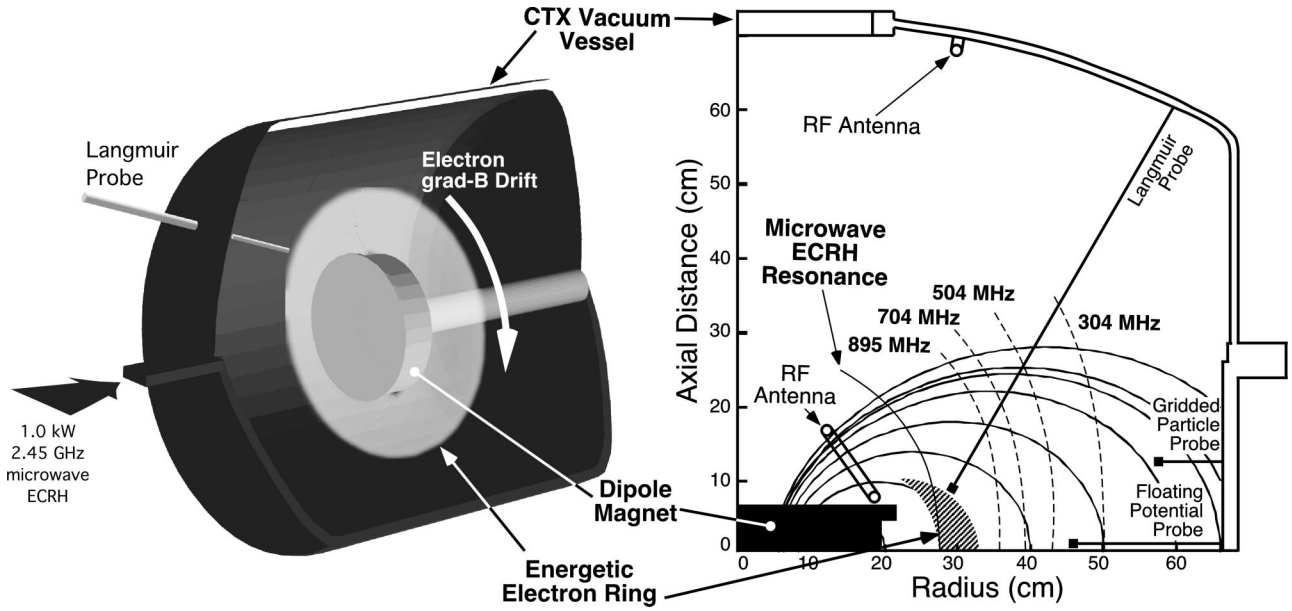

FIG. 1. Illustrations of the Collisionless Terrella Experiment (CTX). The left illustrates a general layout showing the dipole electromagnet inside an aluminum vacuum vessel and an energetic electron ring created by high-power microwave heating. The right shows a quadrant view of the cross-section of the CTX device. Key plasma diagnostics, rf antennas, and locations of electron-cyclotron resonances for selected frequencies used in the experiments are displayed. Locations of the energetic electron ring and microwave resonances are also shown.

of rf fields. Frequency sweeping is characteristic of the nonlinear saturation of the hot electron interchange (HEI) instability in the Collisionless Terrella Experiment (CTX).[3–5] The instability is driven by a non-Maxwellian population of energetic electrons confined by the field of a magnetic dipole. When low-power rf fields are applied, the dynamics of the HEI mode is altered and frequency sweeping is suppressed in a controlled manner.

A self-consistent nonlinear simulation is used to model the growth and saturation of the HEI instability. The simulation reproduces both the global mode structures and the rising tones of the HEI instability.[14] Since the HEI instability has a real frequency that is smaller than the average energetic electron drift frequency, $\omega < \omega_d/2$, only phase-space ''holes'' with rising frequencies can form within a laboratory terrella. Because $\psi \propto 1/L$ and because the magnetic drift frequency is $\omega_d(\mu,\psi) = 3c\mu B(\psi)/e\psi \propto \mu/L^2$, where L is a field-line label equal to the field-line's equatorial radius, phase-space ''holes'' are formed at larger radii and move radially inward as the mode frequency rises. Energetic electrons at higher field and smaller radii are displaced outward adiabatically. The outer wall of the experimental device, which limits the radial extent of the plasma, prevents the formation of phase-space ''clumps.''

We have modified the simulation to include spatially-localized diffusion of the magnetic moments of the energetic electrons due to electron cyclotron resonance heating (ECRH).[17] The diffusion due to cyclotron heating is analogous (but not identical) to the velocity–space diffusion proportional to ν_{eff}^3. The application of rf fields cause cyclotron diffusion in localized radial regions, and $\nu_{\mathrm{eff}}(\psi)$ is nonuniform in phase-space. When cyclotron heating is applied at rf frequencies resonating at radii larger than the radius of peak electron pressure, frequency sweeping stops because the ECRH destroys the phase-space ''holes.'' However, since electron cyclotron heating is localized, we find that frequency-sweeping is not suppressed when the frequency of ECRH heating is adjusted to resonate at the peak of the electron pressure. This is in agreement with the observation of frequency sweeping at the end of the quasi-periodic instability bursts present during the steady microwave discharges of the CTX device.

This paper is organized in the following manner. A description of the experimental device and the applied rf fields is presented in Sec. II. The experimental observations of frequency sweeping suppression are described in Sec. III. In Sec. IV, we describe the modifications to the numerical simulation used to interpret the experimental results. Finally, a discussion and summary of the results is given in Sec. V.

II. EXPERIMENTAL SETUP

In CTX, a dipole electromagnet is suspended mechanically inside an aluminum vacuum vessel 2 cm thick and 140 cm in diameter, Fig. 1. Plasma is created by breaking down and heating hydrogen gas with a high power microwave source, which outputs ~ 1 kW of power at 2.45 GHz. The fundamental microwave resonance is a surface defined by $B_0 \equiv B \simeq 875$ G, which intersects the equatorial plane at $L_0 = 27$ cm. The equatorial cyclotron resonance leads to the creation of an ''artificial radiation belt'' of energetic electrons with energies between 1–60 keV. The measured electron distribution is non-Maxwellian,[4] characteristic of microwave-heated plasmas.[17] During microwave heating, the distribution is characterized by subpopulations of ''cold'' electrons with energies below 200 eV, ''warm'' electrons with energies near 1 keV, and ''hot'' electrons with energies extending beyond 60 keV. Typical microwave discharges are made to last be-

tween 0.5 and 1 s. After the microwave power has been switched off, cold and warm electrons begin to recombine rapidly with ions, whereas hot electrons persist for tens of milliseconds creating a so-called ''afterglow.''

A. Diagnostic equipment

Plasma diagnostics include several Langmuir and high-impedance floating potential probes situated throughout the vacuum vessel (Fig. 1). Diagnostics do not perturb plasma significantly unless they are placed within a few centimeters of the fundamental microwave resonance ($L_0 \sim 27$ cm). A Langmuir probe is typically biased at $V=-100$ V to collect the ion saturation current. High-impedance floating potential probes have a 100 kΩ resistor attached to the tip, as well as a 10 μF bypass capacitor connected before the amplifier to form a high-pass filter with a cutoff of 12 kHz. All probes can be repositioned radially to examine density and potential fluctuations at different flux surfaces. Azimuthal and radial mode structures of observed fluctuations are determined by computing correlations between multiple probes.[14] A krypton proportional counter is used to measure x-ray emissions and characterize energetic electrons energy.

To study the transport of energetic electrons, a movable gridded particle analyzer is employed. It is located 13 cm above the equatorial mid-plane, and consists of a series of grids approximately 1.5 mm apart inside a stainless steel box which has an opening centered on one side. The grids are biased to repel ions and electrons with energies less than 100 eV. Current is collected on a metal plate 0.23 cm^2 and is carried along 50 Ω coaxial cable which is terminated into a 1 kΩ load. The entrance aperture of the probe can be rotated with respect to the local magnetic field vector. During the experiments described here, it was positioned perpendicular to the magnetic field, and the time-averaged energetic electron flux was computed.

B. Magnetostatic rf antennas

Magnetostatic rf antennas installed inside the CTX vacuum vessel, Fig. 1, are used to suppress nonlinear frequency sweeping by exciting low power rf fields. The antennas are constructed from a 50 Ω, 0.25 in. coaxial copper cable, contain one or more breaks in the outer shield of the cable to prevent cancellation of the coaxial currents, and are terminated into a matched load. The antennas were installed at one pole of the dipole and on the outer wall of the vessel. Alumina and glass insulating tubing is used to minimize electrical contact with the plasma. A broad-band rf amplifier, used to generate rf fields, has a peak output of 100 W. The antennas excite low-order cavity resonances of the vacuum vessel in the range of 100 to 1000 MHz. Antennas in both locations suppress frequency sweeping in a similar manner when equal power levels are coupled to the same cavity resonant frequencies.

III. HOT ELECTRON INTERCHANGE AND FREQUENCY SWEEPING SUPPRESSION

As the pressure of energetic electrons confined within the dipole magnetic field increases, plasma becomes unstable to low-frequency hot electron interchange (HEI) instability. Drift-resonant waves ($\omega \sim m\omega_{dh}$) are observed with frequencies shifting upward in time during ECR heating phase and afterglow. By correlating signals measured by multiple probes, it was found that observed waves are (1) flute-like, having no structure along the field lines, (2) propagate azimuthally in the direction of electron ∇B drift, (3) have a broad, rigid radial structure.[3–5,14] Wave amplitudes are observed to be in the range of 100–200 V, with larger amplitudes resulting from more energetic electrons.

During high-power plasma heating, instabilities appear in quasi-periodic bursts 300–700 μs long as shown in Figs. 2 and 3. Typical growth rate of such instability burst is ~ 50 μs with frequency spectrum reaching 3 MHz. In the afterglow, fluctuations are found to be more intense reaching higher frequencies ($f<20$ MHz), due in part to a higher average drift frequency of energetic electrons and the absence of the microwave heating. The rate of frequency sweeping is approximately $\dot{\omega}_n/\omega_n^2 \sim 0.2$ during microwave heating, and $\dot{\omega}_n/\omega_n^2 \sim 2\times 10^{-4}$ during the afterglow.

During the microwave heating phase, the spectrum of observed fluctuations of the quasi-periodic bursts changes from broadband to coherent as the instability develops. This change is well-correlated with modulations of the electron flux to the gridded particle analyzer, which corresponds to the radial expansion of the plasma.[4] It was shown earlier that the wave spectrum observed in the initial phase of the quasi-periodic instability burst [Fig. 4(a)] can lead to global chaos and transport due to the wave–particle resonances being closely spaced in phase-space[4,5] whenever the wave amplitude is above ≈ 75 V. As the electrons are expelled radially beyond $L_0=27$ cm equatorial position, they no longer experience cyclotron heating from high-power microwaves. For these electrons, μ, the first adiabatic invariant, and J, the second adiabatic invariant, are constants of motion. This implies that the ratio $v_\parallel/v_\perp$ increases much more slowly with L than $\sqrt{R}$, and $v_\parallel/v_\perp > \sqrt{R-1}$ criteria for cyclotron diffusion is not satisfied. Here, R is the mirror ratio defined as the ratio of the cyclotron resonant field, $B_0=875$ G, to the equatorial field at a given L. During this phase of the burst a coherent spectrum of waves is observed [Fig. 4(b)] with frequencies rapidly sweeping upward. It also corresponds to diminished radial transport, since the higher frequency coherent waves lead to a chaos that is localized to narrow regions of phase-space (ϕ,ψ). This process essentially creates a radially broadened energetic electron ''disk,'' which, we believe, can support the phase-space ''holes'' on field lines beyond $B=875$ G.

When low-power electron cyclotron resonant rf fields are excited in the range of 100 MHz to 1000 MHz of sufficient intensity and pulse-length, the nonlinear frequency sweeping of resonant interchange modes is suppressed during the microwave heating phase and the afterglow. As soon as rf pulse is discontinued, coherent frequency sweeping reappears. As will be discussed, low-level rf fields that resonate with the cyclotron motion of electrons on outer field lines scatter energetic electrons and cause diffusion of magnetic moments, μ. This diffusion destroys the phase-space

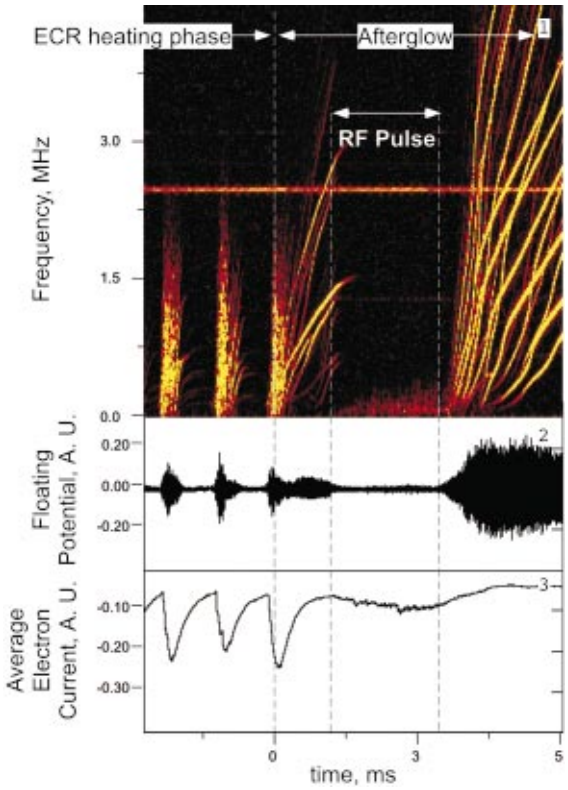

FIG. 2. (Color) Measurement of frequency sweeping suppression during the ''afterglow,'' when a radio frequency pulse of $\omega/2\pi=701$ MHz, 34 W is applied. Electrostatic fluctuations are measured with a floating potential probe (2), and then transformed into a time–frequency domain (1). The gridded particle analyzer located at $L=57$ cm collects current due to energetic electrons (3).

''holes'' required for frequency sweeping to occur at the location of fundamental cyclotron resonance.

Figure 2 displays a typical example of frequency sweeping suppression during the afterglow phase of the discharge.

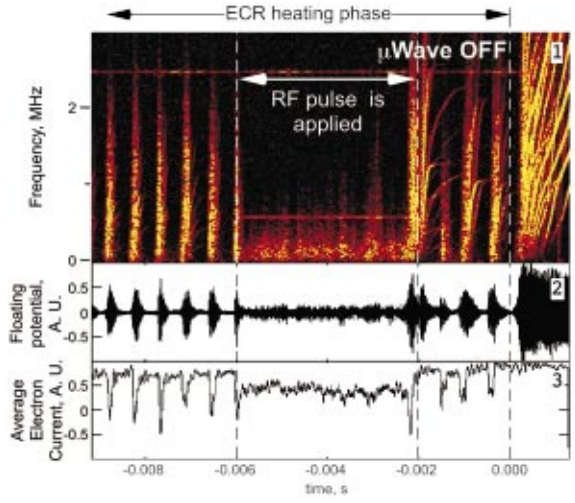

FIG. 3. (Color) An example of frequency-sweeping suppression during ECR heating. Radio frequency fields at $\omega/2\pi=375$ MHz, 16 W are applied. From top to bottom, the plot shows (1) a time-frequency spectrogram of measured plasma fluctuations, (2) plasma floating potential fluctuations, (3) hot electron current to the gridded particle probe located at $L=55$ cm.

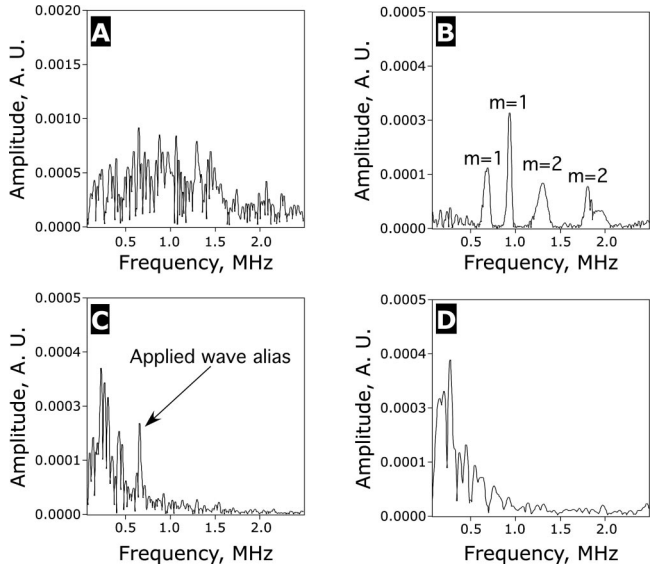

FIG. 4. Spectral characteristics of the observed fluctuations are presented. (a) Initial chaotic phase of the HEI instability burst during ECR heating. (b) Coherent phase of the HEI instability burst during ECR heating. (c) and (d) present spectra of turbulent low frequency fluctuations induced by rf fields during the ECR heating phase and the afterglow, respectively.

At low power settings ($P\approx 10$ W), the high azimuthal modes ($m=2,3$) are suppressed before the low azimuthal modes ($m=1$). The rate of frequency sweeping is observed to decrease at the very onset of the rf pulse. As the power is increased ($P=30$ W), frequency sweeping is arrested until the rf fields are switched off. Frequency sweeping is also suppressed during the ECR heating phase of the discharge, Figs. 3 and 5. Figure 3 shows a typical example of suppression during the heating phase for a 16 W pulse at $\omega/2\pi=375$ MHz. Figure 5 shows the intensity of measured fluctuations in a frequency band 1.9 MHz$\leqslant f\leqslant$2.1 MHz, normalized to the intensity below that band, as a function of applied rf power. This provides a convenient measure of frequency sweeping during the 300–700 μs quasi-periodic instability bursts.

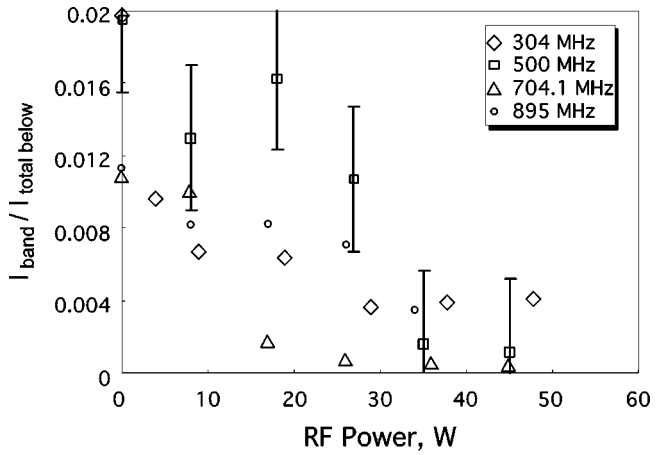

FIG. 5. Frequency sweeping suppression during the ECRH phase. $I_{\text{band}}/I_{\text{total below}}$ represents the amount of frequency-sweeping as a function of the power of applied rf fields at various frequencies.

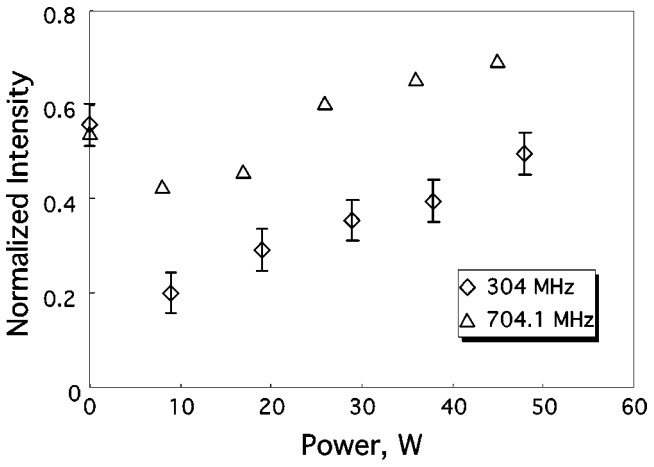

FIG. 6. Intensity within a frequency band 0.2 MHz$\leqslant f \leqslant$0.4 MHz normalized to the intensity below that band, $f<0.4$ MHz, as a function of the power of applied rf fields is shown. This provides a measure of the amount of low frequency turbulent fluctuations induced by the applied rf fields during the suppression of frequency-sweeping.

During the suppression of frequency sweeping, the low frequency turbulent fluctuations are induced by the applied fields. They have broadband spectrum [Figs. 4(c) and 4(d)] similar to the one observed during the chaotic phase of the quasiperiodic HEI instability burst, albeit lower amplitude and more localized toward the low frequencies. The intensity of the induced low frequency fluctuations is well-correlated with the enhanced energetic electron transport as seen in Figs. 6 and 7, consistent with the quasi-linear theory predictions.[4] Since the power levels of the applied fields are low ($<5\%$ of the main microwave heating power) and because the nonlinear frequency sweeping reappears once rf pulse is switched off, the applied fields apparently do not create large changes in the distribution of energetic electrons. Instead, the effective collisionality of the system, ν_{eff}, is increased corresponding to the presence of scattering from cyclotron resonance with the applied rf fields.

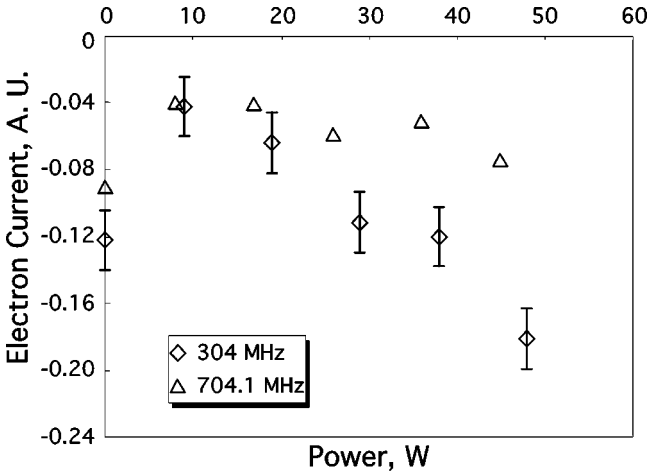

FIG. 7. The average energetic electron current to the gridded particle analyzer as a function of the power of applied rf fields is plotted. It is well-correlated with the induced low frequency turbulent fluctuations in Fig. 6.

IV. NUMERICAL SIMULATION OF FREQUENCY SWEEPING SUPPRESSION

Self-consistent nonlinear numerical simulation is used to study the HEI instability and interpret the results of experimental observations.[12,14] The simulation reproduces nonlinear frequency sweeping and the radial structure of the modes. It also illustrates spontaneous creation and inward propagation of phase-space "holes," [13] Fig. 8, which are believed to be an essential feature of the instability saturation process and nonlinear frequency sweeping.[7] The simulation explicitly solves for the evolution of cold ion and energetic electron number densities and the electrostatic potential, Φ, on the (ψ,φ) plane. (ψ,φ) are the canonical coordinates of the electrons' guiding-center drift Hamiltonian (i.e., the electron phase-space) and the magnetic coordinates of the dipole, $\mathbf{B}=\nabla\psi\times\nabla\varphi$.[8] Plasma $\mathbf{E}\times\mathbf{B}$ and ion polarization drifts, and energetic electron magnetic drifts determine particle dynamics, and Poisson's equation in magnetic coordinates determines the nonlinear evolution of the potential. Bounce-averaged distribution function $F(\mu,\psi,\phi,t)$ is used to describe the dynamics of energetic electrons. Here, $\mu \equiv m_e v_\perp^2/2B$ is the magnetic moment, m_e is the electron mass, and B is the local strength of the magnetic field. The effects of parallel motion along the magnetic field are ignored, and $J=0$.

In simulations presented here, seven distinct hot electron "fluids" were used to describe the phase-space flows occurring for different values of μ ($0.15\mu_0$, $0.3\mu_0$, $0.5\mu_0$, $0.75\mu_0$, $1.0\mu_0$, $1.25\mu_0$, $1.5\mu_0$). Here $\mu_0=9\times10^{-12}$ erg/G is the characteristic hot electron magnetic moment for CTX. Since electrons at different energies have different drift velocities at different radii, wave–particle resonances occur simultaneously at several radii and electron energies, $\omega=\omega_d(\mu,\psi)$. These resonances correspond to the locations of the phase-space "holes." Figure 8 shows the phase-space evolution of one energy group of hot electrons with $\mu=0.75\mu_0$. As the instability develops, phase-space "holes" are initiated within different hot electron fluids at different times, with low μ electrons developing the structures first. As the mode frequency increases, "holes" are created at higher energies and always move inward from the outer edge. At any instant, the phase-space "holes" create a non-smooth distribution within each phase-plane (at constant μ) and between phase-planes (at constant ψ and φ).

A. Modeling ECR diffusion

The presence of applied electron-cyclotron resonant fields are modeled in the simulation as causing diffusion of energetic electrons by stochastic scattering of μ. For simplicity, the diffusion rate is taken to be independent of μ, uniform in azimuthal angle, and vary only in radius, ψ. The numerical procedures (described more fully in Refs. 12 and 14) are modified according to

$$\frac{\partial}{\partial t}F(\mu,\psi,\varphi,t)+\cdots=D(\psi,t)\frac{\partial^2}{\partial\mu^2}(F-F^*). \tag{1}$$

Here, $D(\psi)$ is the magnitude of simulated diffusion, and $F^*(\mu)$ is a reference distribution function that is defined so

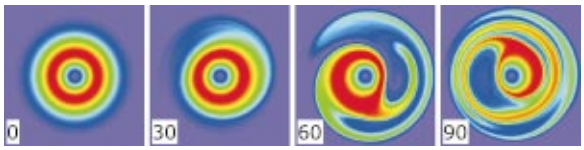

FIG. 8. (Color) Coherent structures in phase-space—the phase-space ''holes''—as illustrated by the self-consistent nonlinear numerical simulation used in CTX. The time evolution of phase-space is shown for one energy group of hot electrons $-0.75\mu_0$. Red indicates the maximum in particles density, purple—minimum. As the instability develops, vacuum bubbles are observed to form on the outer flux surfaces and propagate inward.

that ECR diffusion leaves unchanged the initial electron energy distribution while smoothing relative gradients in the μ-direction. The numerical proceedure for ECRH preserves the total energetic electron number within each flux tube.

This form of velocity-space diffusion is related to the effective collisionality specified in Berk's formulation [Ref. 7, Eq. (14)]; however, the physical processes differ. In Berk's formulation, stochastic scattering of a particle's velocity moved particles *within a single phase-space plane*. The lifetimes of phase-space ''holes'' and ''clumps'' were limited by the slow diffusion and smoothing of nearby phase-space density in the (v,x) [or equivalently (Ω,ξ)] phase-plane. In contrast, the velocity-space diffusion caused by ECRH in a dipole confined plasma causes stochastic scattering of the electron's magnetic moments. This causes diffusion that *connects different but neighboring phase-space planes* each represented by a different value of μ. ECRH changes the dimensionality of the energetic electron dynamics. Without ECR fields, low-frequency interchange modes cause motion in multiple (ψ,φ) phase-planes defined by constant values of μ. When ECRH is added to the low-frequency potential of the interchange mode, electron dynamics requires treating the time evolution of phase-space density in (at least) two velocity–space actions, $\partial F(\mu,\psi,\varphi,t)/\partial t \neq 0$. This is accomplished numerically with a time-splitting sequence of solutions of Eq. (6) of Ref. 14 combined with a fully-implicit solution of Eq. (1).

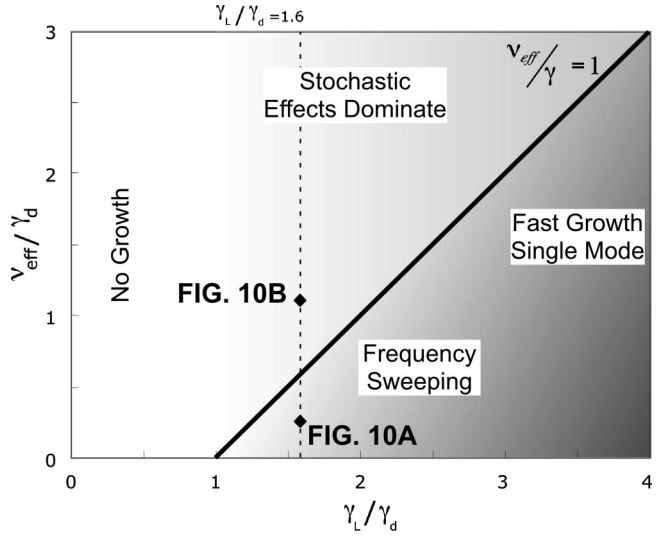

FIG. 9. Possible ways for interchange instability to develop as prescribed by Berk and co-authors. By changing the effective collisionality of the system, we destroy the phase-space ''holes'' and arrest the frequency-sweeping as shown in Fig. 10.

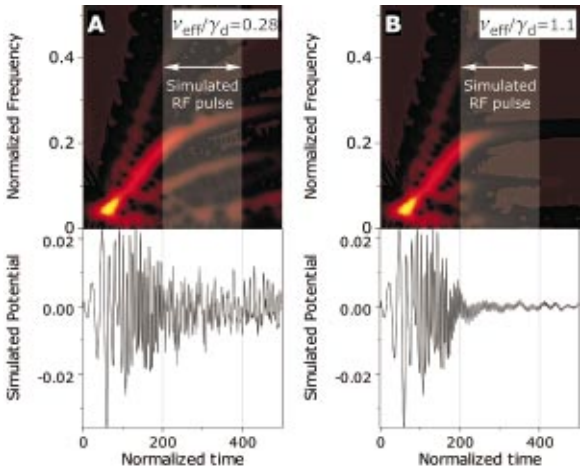

FIG. 10. (Color) Numerical simulation of frequency sweeping suppression for the case of $\gamma_L/\gamma_d = 1.6$. Simulated rf pulse is applied from $t = 200$ t.u. to $t = 400$ t.u. The simulated potential and the time–frequency spectrogram are shown.

Although the physical processes of velocity–space diffusion modeled by Berk and co-workers[7] and by this article are different, their effects on frequency-sweeping are comparable. We believe this is because the particle resonant frequency scales strongly with μ and the phase-space gradients in the μ direction are comparable to those in the ψ direction. Using the relationship $\omega_{dh} = 3c\mu B(\psi)/e\psi$ to relate the drift frequency of energetic electrons to the magnetic moment, the diffusion operator in Eq. (1) can be recast in the form $\nu_{\mathrm{eff}}^3(\partial^2/\partial\omega_d^2)(F-F^*)$, where $\nu_{\mathrm{eff}}^3(\psi) \equiv 9D(\psi)(cB/e\psi)^2$ is the effective diffusion coefficient for resonant particles. Since

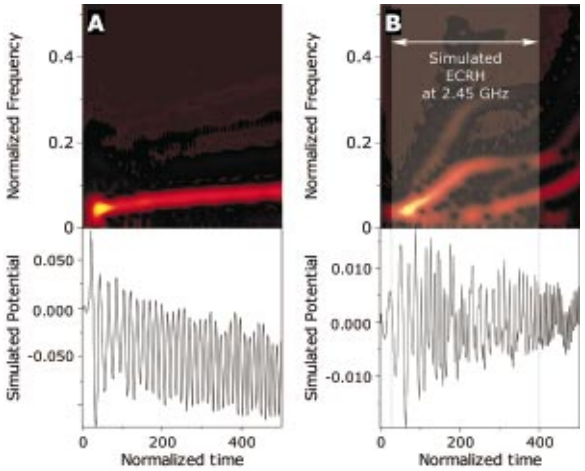

FIG. 11. (Color) Other effects reproduced by the numerical simulation. (a) Numerical simulation of the HEI instability for $\gamma_L/\gamma_d > 6$. The mode saturates into a BGK-like structure without significant frequency-sweeping, as predicted by the nonlinear theory. (b) Numerical simulation of ECRH at 2.45 GHz. Simulated rf pulse is applied from $t = 25$ t.u. to $t = 400$ t.u. The simulated potential and the time–frequency spectrogram are shown in both cases.

ECRH in a dipole creates a nonuniform ν_{eff}, we define $\langle \nu_{\text{eff}} \rangle$ to be the flux average of $\nu_{\text{eff}}(\psi)$ which simplifies the comparison with Ref. 7.

Finally, note that the radial variation of $D(\psi)$ (or ν_{eff}^3) depends upon the frequency of the applied microwave or rf fields. The location of particle diffusion in the μ direction changes by adjusting the frequency of the applied cyclotron resonant fields. We model $D(\psi)$ to be largest at the equatorial cyclotron resonance and to vanish for flux surfaces differing by factors exceeding $\pm 10\%$ to $\pm 25\%$. By modeling the initial radial profile of the trapped electrons to represent (within experimental uncertainties) measurements, the only adjustable parameters in the model are the form of $D(\psi)$ and a constant, nonresonant dissipation that gradually damps the potential at a rate γ_d described in Ref. 14.

B. Discussion of numerical results

According to Berk and co-workers,[7] two criteria must be met for coherent hole–clump structures and frequency-sweeping phenomena to develop: (1) the system must be near the linear instability threshold $\gamma_L < 2.5\gamma_d$, and (2) the resonant particles must be collisionless, $\nu_{\text{eff}} \leqslant \gamma_L - \gamma_d$. Our numerical simulations of the HEI instability support these criteria. Examples are summarized in Fig. 9 which shows the conditions for frequency-sweeping and displays representative results from the numerical simulation. Figure 10 shows the computed potential fluctuations when the nonresonant damping rate γ_d was adjusted so that $\gamma_L/\gamma_d = 1.6$. As the magnitude of the diffusion coefficient D is increased, the ratio $\langle \nu_{\text{eff}} \rangle / \gamma_d$ is changed from $\langle \nu_{\text{eff}} \rangle / \gamma_d = 0.28$ [Fig. 10(a)] to $\langle \nu_{\text{eff}} \rangle / \gamma_d = 1.1$ [Fig. 10(b)]. The frequency-sweeping is diminished in accordance with predictions of Ref. 7. The examination of the computed electron phase-space shows that frequency sweeping is suppressed when the ECR diffusion destroys the phase-space ''holes.'' The simulation also shows the absence of frequency-sweeping when the instability is far from marginal stability. For example, when $\gamma_L > 6\gamma_d$, frequency-sweeping does not occur [Fig. 11(a)], and the HEI instability saturates as a single coherent nonlinear mode.

The rate of rf diffusion, D, required in the simulation to suppress frequency-sweeping is comparable to the diffusion induced by the applied rf fields. When Eq. (1) is integrated over particle's energy, $\mu B(\psi)$, and plasma volume, we find that rf power required to suppress frequency sweeping in Fig. 10(b) is 50 W with reasonable estimates of electron profiles and $-\int d\mu \partial/\partial\mu (F - F^*) \leqslant N_h/2\mu_0$. Additionally, the rf diffusion rate used in the simulation is comparable to the bounce-averaged diffusion rate[17] computed using the vacuum fields estimated from the quality of the cavity resonance. With $Q \sim 300$, the cavity electric field, $E_\perp$, is approximately 20 V/cm for 50 W.

We find it significant that the simulated rf diffusion induced by the 2.45 GHz microwaves at a 1 kW level does not suppress frequency-sweeping when $D(\psi)$ is localized at the peak electron pressure, Fig. 11(b). The radial location of the primary microwave heating allows phase-space ''holes'' to continue to form at larger radii. As the frequency increases and the ''holes'' move to smaller radii, the high-power ECRH is seen to limit, but not suppress, the range of frequency-sweeping.

Although the modified nonlinear simulation reproduces frequency-sweeping suppression due to ECRH diffusion, some phenomena seen in the laboratory are not reproduced well by the simulation nor can the simulation properly model the long-term evolution of the plasma. For example, the induced low frequency fluctuations during the suppression of frequency-sweeping correlated with the enhanced transport of energetic electrons are not reproduced by the simulations.

V. SUMMARY

Frequency-sweeping associated with the nonlinear saturation of the hot electron interchange instability (HEI) was suppressed upon the application of rf fields. Frequency-sweeping is characteristic of the evolution of HEI modes excited by energetic electrons trapped within a dipole-confined plasma. The low-level applied rf fields induced stochastic diffusion at localized regions by electron cyclotron resonance. Using a self-consistent, nonlinear simulation, we show that the observed frequency sweeping suppression results from the destruction of phase-space ''holes'' as predicted by a theory of Berk and co-workers.[7]

ACKNOWLEDGMENTS

We gratefully acknowledge the support of AFSOR Grants No. F49620-97-0425 and No. F49620-97-1-0026 and U.S. DOE Grant No. DE-FG02-00ER54585.

[1] M. Schulz and L. J. Lanzerotti, *Particle Diffusion in the Radiation Belts* (Springer-Verlag, New York, 1974).
[2] A. Fasoli, D. Borba, B. Breizman *et al.*, Phys. Plasmas **7**, 1816 (2000).
[3] H. P. Warren and M. E. Mauel, Phys. Rev. Lett. **74**, 1351 (1995).
[4] H. P. Warren and M. E. Mauel, Phys. Plasmas **2**, 4185 (1995).
[5] H. P. Warren, M. E. Mauel, D. Brennan, and S. Taromina, Phys. Plasmas **3**, 2143 (1996).
[6] H. P. Warren, A. Bhattachargee, and M. E. Mauel, Geophys. Res. Lett. **19**, 941 (1992).
[7] H. L. Berk, B. N. Breizman, J. Candy *et al.*, Phys. Plasmas **6**, 3102 (1999).
[8] A. H. Boozer, Phys. Fluids **23**, 904 (1980).
[9] H. L. Berk, B. N. Breizman, and M. Pekker, Phys. Rev. Lett. **76**, 1256 (1996).
[10] B. N. Breizman, H. L. Berk, M. S. Pekker *et al.*, Phys. Plasmas **4**, 1559 (1997).
[11] N. A. Krall, Phys. Fluids **9**, 820 (1966).
[12] M. E. Mauel, J. Phys. IV **7**, 307 (1997).
[13] D. Maslovsky, M. Mauel, and B. Levitt, IEEE Trans. Plasma Sci. **30**, 8 (2002).
[14] B. Levitt, D. Maslovsky, and M. Mauel, Phys. Plasmas **9**, 2507 (2002).
[15] A. Fasoli, B. N. Breizman, D. Borba *et al.*, Phys. Rev. Lett. **81**, 5564 (1998).
[16] R. F. Heeter, A. F. Fasoli, and S. E. Sharapov, Phys. Rev. Lett. **85**, 3177 (2000).
[17] M. E. Mauel, Phys. Fluids **27**, 2899 (1984).